Anuário do Instituto de Geociências
Universidade Federal do Rio de Janeiro
https://revistas.ufrj.br/index.php/aigeo/

ISSN 0101-9759
e-ISSN 1982-3908

GEOLOGY

Geological and Industrial Characterization of the Mylonite Belonging to the Granja Complex, Morrinhos - CE

Caracterização Geológica e Industrial do Milonito Pertencente ao Complexo Granja, Morrinhos – CE

Davi Henrick Veras Diógenes[1] & Irani Clezar Mattos[2]

[1] Universidade Estadual do Ceará, Departamento de Geografia, Fortaleza, CE, Brasil
[2] Universidade Federal do Ceará, Departamento de Geologia, Fortaleza, CE, Brasil
E-mails: davihenrick@gmail.com; irani.mattos@ufc.br

Abstract

Considering that establishing an ornamental stone deposit requires various preliminary studies, this research aimed to identify the potential of a mylonite belonging to the Granja Metamorphic Complex in the Médio Coreaú Domain. To this end, geological mapping, technological characterization, and reuse studies were conducted. The technological characterization considered both national standards, developed by ABNT, and European and American standards. For determining the reuse options for the cutting and dismantling waste of the material, tests were conducted for its use as a partial replacement for coarse aggregate in concrete, as eco-filler, and for the production of artificial agglomerated stone. In the end, in addition to understanding the geological history of the rock, it was possible to determine its safe use as an ornamental stone and the best ways to utilize the waste.

Keywords: Ornamental stones; Technological characterization; Reuse

Resumo

Considerando que para se consolidar uma jazida de rochas ornamentais são necessários diversos estudos prévios, na presente pesquisa buscou-se identificar o potencial de um milonito pertencente ao complexo metamórfico Granja no Domínio Médio Coreaú. Para tanto, foram realizados mapeamento geológico, caracterização tecnológica e estudos de reaproveitamento. A caracterização tecnológica levou em conta tanto normativas nacionais, elaboradas pela ABNT, quanto europeias e estadunidenses. Já para a determinação das formas de reaproveitamento do rejeito de corte e desmonte do material, foram realizados testes para a utilização em substituição parcial de agregado graúdo em concreto, como ecofiller e para a produção de rocha artificial aglomerada. Ao fim, além de conhecer a história geológica da rocha, foi possível determinar sua segura utilização como rocha ornamental e melhores formas de aproveitamento de rejeito.

Palavras-chave: Rochas ornamentais; Caracterização tecnológica; Reaproveitamento

Received: November 9, 2024; Accepted: March 26, 2025

1 Introduction

The use of rocks has historically been associated with factors such as durability, strength, and beauty, and currently plays important roles in various applications in civil construction, from decoration and protection to temperature reduction and even structural support. However, to ensure the proper use of these materials, it is essential to conduct a detailed characterization that considers all factors that may influence the rock's behavior and performance under the most adverse conditions.

This study aims to identify the exploitation potential of ornamental rocks through the geological and physical-mechanical characteristics of a mylonite extracted in the municipality of Morrinhos, located in the northwest region of the state of Ceará. The use of stone materials has historically been linked to factors such as durability and beauty; today, this type of product plays a fundamental role in various applications in civil construction, from space decoration to the construction of support structures. However, to ensure the appropriate use of these materials, a detailed characterization is essential, taking into account all factors that may influence the rock's behavior.

This study proposes a comprehensive analysis of the mylonite, focusing on its geological history and ornamental application. To this end, the work includes an evaluation ranging from the geological characteristics of the rock to its strength properties, methods of use, conservation, and possibilities for reuse.

In order to establish a solid foundation for the analyses, an extensive literature review was conducted to support all stages of the study. The analyses were divided into major thematic areas: Mapping, Technological Characterization, Geochemistry, Alterability, and Reuse. The creation of a geological map at a local scale, based on fieldwork, is not only useful for understanding the processes that formed the rock but also capable of identifying facies variations to indicate the distribution of the rock body to be exploited.

The determination of the physical-mechanical parameters of a rock is highly relevant for understanding its potential uses, with analyses in this part of the study based on national and international standards. In this context, uniaxial compressive strength tests, flexural strength tests, abrasive wear resistance tests, hard-body impact resistance tests, determination of physical indices, and capillary rise rate tests were conducted.

Understanding the rock's chemical characteristics not only contributes to comprehending its geological evolution but also provides important data about its possible uses and

limitations. The study areas of Alterability and Conservability are essential for determining the best practices for using and maintaining the stone material, as they specifically address the rock's resistance to alterations. For determining these parameters, tests were conducted on wave propagation velocity, stain resistance, chemical attack resistance, static contact angle with water, and sulfur dioxide exposure resistance.

Finally, in alignment with current environmental concerns, analyses were conducted on the reuse of waste generated during the mining of the mylonite, aiming to identify possible applications. For this purpose, the material was tested for use as aggregate in concrete, eco-filler, and artificial agglomerated stone. Thus, this study addresses the rock from its geological origin to its final use and the reuse of its waste, providing a comprehensive and integrated view of its potential.

2 Study Area

The analyzed rock is located in the municipality of Morrinhos, in the northwestern region of the state of Ceará, about 208 kilometers from Fortaleza. Access to the area can be made from Fortaleza by first traveling 100 kilometers on the CE-085 highway, then continuing on the CE-354 highway for another 108 kilometers to the center of Morrinhos. The study area is specifically located approximately 8 kilometers southwest of the town center in a straight line.

The locality is within the Bela Cruz geological map (AS.24-Y-D-I) (Pinéo et al. 2018) and borders the municipalities of Marco, Santana do Acaraú, Itarema, Amontada, Acaraú, and Senador Sá (Figure 1). It is situated in the morphotectonic domain of Médio Coreaú, a region of high geological complexity, with extensive folded belts and a large number of shear zones (Santos et al. 2007), as discussed in section 4.

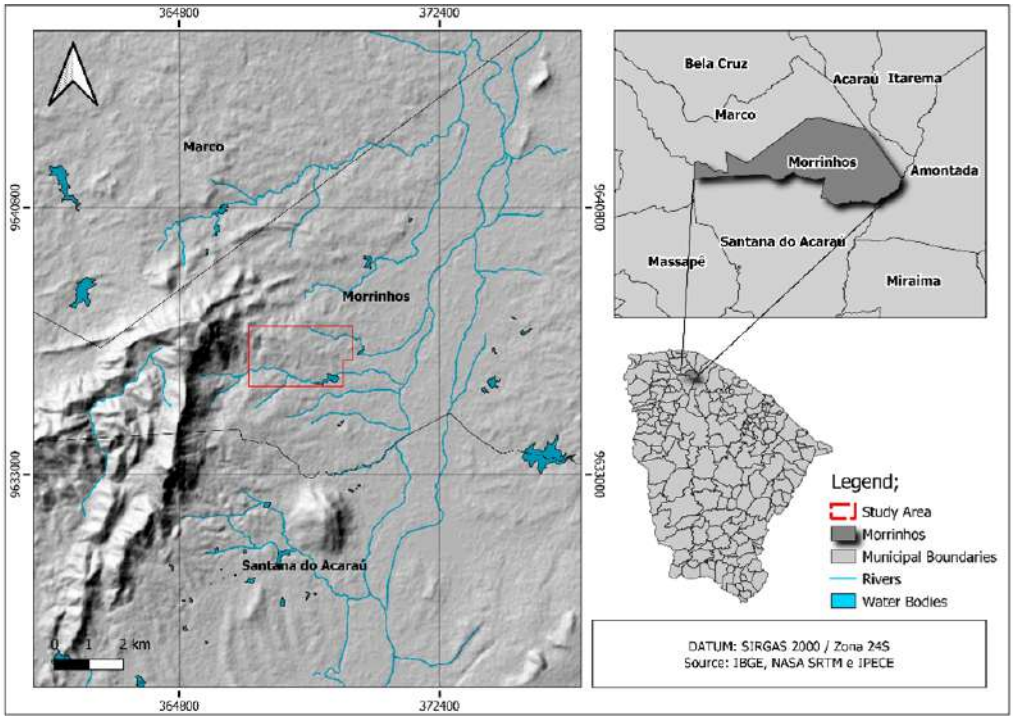

Figure 1 Location map of the study area.

3 Methodology and Data

This study aimed to characterize the mylonitic rock by assessing its potential for extraction and use as an ornamental stone. Field mapping and various technical-scientific analyses were conducted to describe both the geological characteristics of the rock's origin and its technical aspects of strength, as well as potential uses for its waste.

The geological characterization of the mylonite was initially performed through geological mapping, petrography, and chemical analysis. In the following stage, the technological characterization of the rock was based on methodologies outlined by the standards of the Brazilian Association of Technical Standards (ABNT), European Standards (EN), and the American Society for Testing and Materials (ASTM).

The last two stages were conservability analysis, which included studies on rock conservation and defect mitigation, and waste reuse analysis. Although this latter product has not yet been developed, in today's context of environmental concerns, identifying possible reuse methods is essential before establishing the mine to envision sustainable solutions.

Geological mapping was conducted at a detailed scale (1:20,000), allowing the delimitation of facies variations of the outcropping rocks in the region. The samples collected during mapping were described both macroscopically and microscopically, and analyzed using X-ray diffraction, scanning electron microscopy (SEM), and

lithogeochemistry via ICP-OES. The tests were performed according to specific standards, as presented in Table 1.

Table 1 Laboratory tests conducted and their respective standards.

Tests	Standards		References
	ABNT	ASTM or EN	
Technological Characterization			
Slip Resistance	NBR 16959	EN 14231	ABNT (2021a)
Physical Indices	NBR 15845-2	–	ABNT (2015b)
Uniaxial Compressive Strength	NBR 15845-5	C-615	ABNT (2015c)
Flexural Strength	NBR 15845-6	C-615	ABNT (2015d)

Table 1 Cont.

Tests	Standards		References
	ABNT	ASTM or EN	
Hard Body Impact Resistance	NBR 15845-8	C-170	ABNT (2015e)
Water Absorption by Capillarity	–	EN 1925	EN (2000)
Amsler Abrasive Wear	NBR 12042	C-241	ABNT (1992)
Alterability			
Chemical Resistance	NBR 16596	–	ABNT (2017)
Stain Resistance	NBR 10545-14	–	ABNT (2018)
Static Contact Angle	–	EN 14205	EN (2010)
Resistance to SO2	–	EN 13919	EN (2003)
Wave Speed	–	D-2845	ASTM (2015)
Reuse			
Grain Size	NBR NM 248	–	ABNT (2003)
Density	NBR 9776	–	ABNT (1987)
Unit Weight	NBR 16972	–	ABNT (2021b)
Shape Index	NBR 7809	–	ABNT (2019a)
Wave Speed in Concrete	NBR 8802	–	ABNT (2019b)
Compressive Strength	NBR 5738	–	ABNT (2015f)

In line with recent efforts to associate development with sustainability, analyses were conducted to determine the potential for reusing mylonite waste in three different ways:

(i) as coarse aggregate in concrete, (ii) as eco-filler, and (iii) as artificial agglomerated stone.

Initially, the rock was crushed and its granulometry determined. It was then classified according to NBR 7211 standards into coarse aggregate, fine aggregate, and fine powder. The coarse aggregate portion was tested to determine its shape index, specific mass, and unit mass with the aim of using it as a replacement for conventional gravel in concrete composition.

The fine aggregate fraction was used to produce samples of artificial agglomerated stone, which were characterized by their physical indices and abrasion resistance. Finally, the fine powder was used as a partial cement substitute in the concrete mixture.

For casting the concrete test specimens, the methodology of the Brazilian Portland Cement Association (ABCP) was followed, with a slump cone test yielding a range between 40-60mm. The mixture proportion used was 2 kg of gravel, 1.8 kg of sand, 1 kg of cement, and 450 ml of water. Conventional gravel was replaced with waste aggregate at rates of 33%, 66%, and 100%. To test the use of eco-filler, 5% of the cement was replaced with rock powder, similar to studies by Queiróz (2017) and Gesta (2019).

For the production of artificial stone, epoxy resin SQ-2001 was used with hardener SQ- 3154-BB, while the rock component used the fraction defined by ABNT NBR 7211 as fine aggregate. The mixture was prepared at a 70% rock to 30% resin ratio, using the vacuum vibration method to prevent bubble entrapment, similar to the methods employed by Aguiar et al. (2017), Lee et al. (2008), and Agrizzi et al. (2019).

4 Geology

The mapping of the study area was conducted at a detailed scale (1:20,000), where the facies of the present lithologies were identified with the purpose of delineating the economically mineral-interest body. Migmatitic rocks belonging to the Granja Complex were recorded, covering over 60%, along with quartzites from the São Joaquim Formation, which occupy the remaining 30% of the study area.

In the rock formed by the mylonitization of migmatites from the Granja Complex, outcrops extend beyond 50 meters in length and are generally found within migmatites with less intense mylonitization. As a result of the mapping and petrographic analysis (ABNT, 2015a), Figure 2 presents a geological map with the division of facies observed in the field, indicating their variations to aid in selecting the best extraction fronts. The mylonite outcrops generally occur in elongated shapes, with their extension following the same orientation as mineral stretching.

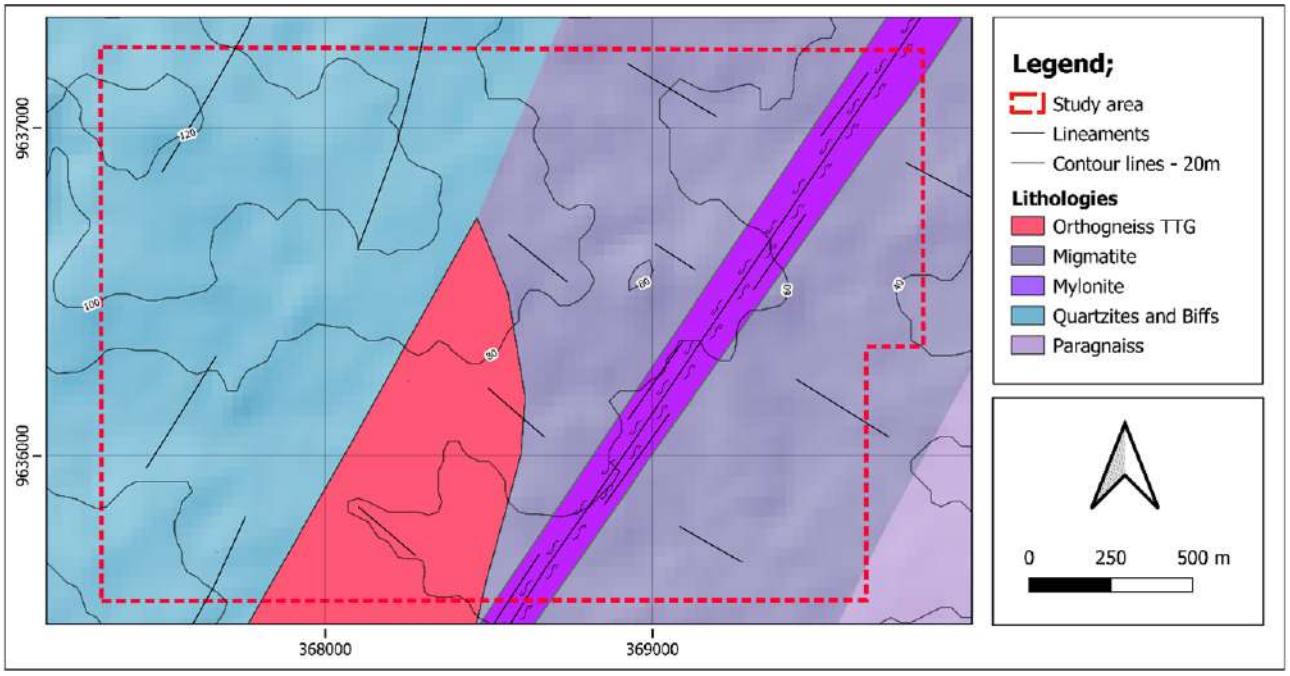

Figure 2 Geological map of the study area.

Variations in composition or the intensity of mylonitization along the shear zone have produced rocks with differing textural and, consequently, aesthetic characteristics. These differences are evident in composition, texture, and grain size, which can lead to either an increase or decrease in the rock's value as an ornamental piece. The dark green mylonite (intensely mylonitized), with few phenocrysts, outcrops in the central-southern portion of the study area, bordered by gneisses with less intense mylonitization.

In the northeastern portion of the area, mylonite outcrops can also be observed, but they are coarser-grained and contain a greater number of phenocrysts. When comparing the facies geological map (result of the present mapping) with the geological map of the state of Ceará (Pinéo & Palheta 2021), a cartographic shift in the position of the contact between the Granja Complex and the São Joaquim Formation can be observed, with the former now covering a larger area than the latter.

From the western to the eastern portion of the study area, quartzites belonging to the São Joaquim Formation are visible. These quartzites exhibit strong fracturing at 58°(NE) and have an impure composition with a large number of micaceous minerals, as presented by Nunes (2018). The soil associated with this lithology has a white coloration and is composed mainly of quartz, resembling beach sand. At times, the whiteness of these soils is interrupted by regions of intense red with high iron concentration, with lateritic characteristics, stockwork, and bands associated with the iron formations that also comprise the São Joaquim Formation.

The petrographic analysis shows that the mineralogy of the quartzite consists of quartz (91%), muscovite (6%), K-feldspar (2%), with accessory minerals including zircon, apatite, and sericite. It has a mylonitic texture and a banded structure, where the grains predominantly exhibit serrated contacts between each other. Straight contacts can also be observed in the interaction between quartz and muscovite grains. The microfractures lack infill and are predominantly within the size range of 0.04 to 0.12 mm, mostly of the intragranular type.

In contact with the quartzites is the TTG orthogneiss. Macroscopically, this rock has a massive structure and a hololeucocratic coloration, displaying indicators of fusion and a high fracture rate, with two main fracture sets oriented at 90° and 160°. In some fractures or as clusters, masses of epidote can be identified with a typical pistachio-green coloration that contrasts with the color of the rock (Figure 3).

In the section, the mineralogy of the TTG orthogneiss is composed of quartz (40%), plagioclase (46%), K-feldspar (4%), epidote (6%), chlorite (3%), and zircon (<1%) as an accessory. These minerals predominantly exhibit concave-convex and serrated contacts.

The plagioclase grains, which have a significant percentage, show advanced alteration, with most of the grains being clay-rich.

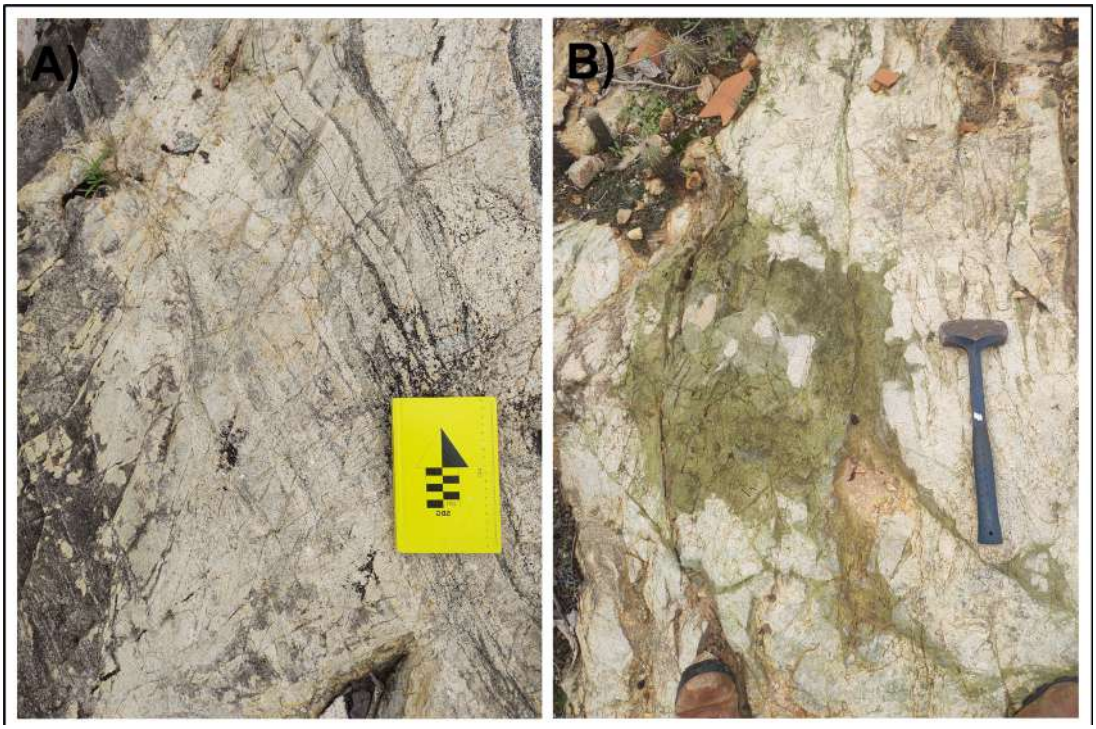

Figure 3 A. Macroscopic image of the outcrop of TTG orthogneiss; B. Accumulation of epidote filling fractures and cavities.

Due to the high concentration of plagioclase, the absence of mafic minerals, and the color index, it was possible to classify the rock as tonalitic in composition, supporting the classification adopted by Silva (2017) of TTG orthogneiss. Portions with a higher concentration of stromatic leucosome are also observed; these leucosomes occur in the form of elevated reliefs in a rock with a slightly pink coloration.

The protolith of the rock in question is classified as migmatite. Compared to TTG orthogneiss, there is a significant color difference due to the increased amount of mafic minerals, resulting in a mesocratic coloration. The rock has a grayish color, displaying typical features of the partial melting process, where diatexite and metatexite portions can be observed.

Macroscopically, the rock exhibits a banded structure and may or may not present a mylonitic texture, depending on the proximity to the shear zone. A more greenish coloration can also be observed (Figure 4 A-B). In the portions farther from the shear zone, an increase in the intensity of folding is also noticeable, particularly in Z- and M- type folds.

Several fractures were identified, with orientations ranging from 90° to 160°, which may or may not show filling by chlorite. Unlike TTG migmatite, large masses or clusters of chlorite are not identified, which may be due to two possible causes. One is the lower amount of plagioclase in its composition compared to TTG migmatite, where these plagioclases underwent a process of saussuritization followed by chloritization. The second cause may be related to reactivation processes of the shear zone, where masses of chlorite were incorporated into the banding of the rock and later, to a lesser extent, dissolved and reprecipitated, filling fractures.

With the mylonitization of the migmatite, a mylonitic texture was generated, identifiable in the form of two main lenses that are located along the shear zone, bordered by protomylonitic rocks. It was not possible to identify defined contacts between the protomylonite and the mylonite, as one grades into the other with changes in the intensity of mylonitization or in the granulation of the protolith.

The rock has a dark green coloration and a very fine matrix with white porphyroblasts that can reach up to 3 cm (Figure 4 C-D). Similar to the protomylonites, sigmoidal structures and stretching lineations indicate a sinistral mylonitic deformation. At the outcrop scale, fractures with a preferred orientation of 120° filled with dark vitrified material and angular rock fragments can be observed.

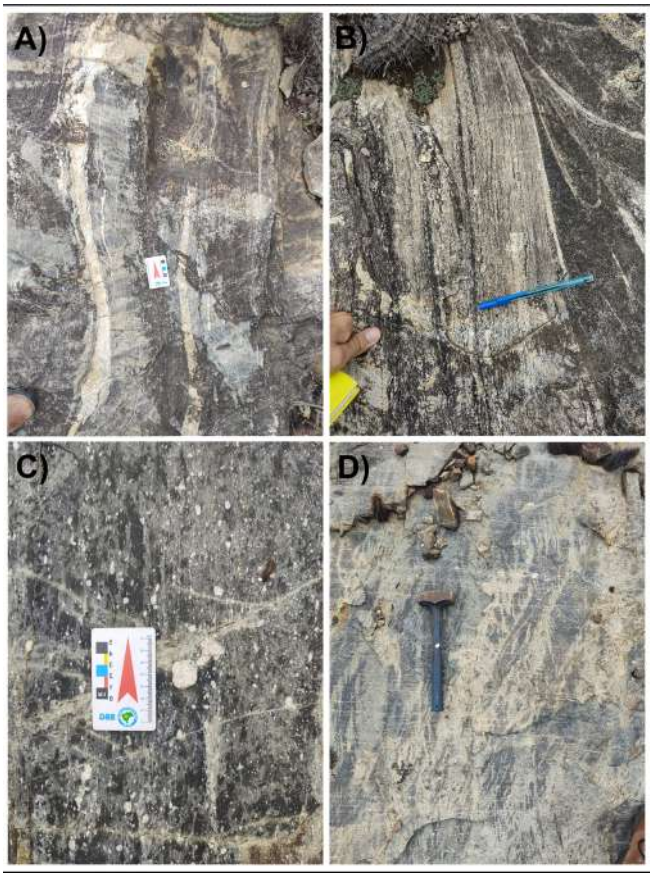

Figure 4 A-B. Macroscopic image of the migmatite outcrop; C-D. Images of the studied mylonite in outcrop.

Microscopically, the rock's mineralogy consists of quartz, plagioclase, K-feldspar, biotite, chlorite, and zircon, with accessories including apatite, monazite, epidote, and garnet. The first three minerals occur as porphyroblasts with dimensions ranging from 0.08 to 6.22 mm, displaying sigmoidal characteristics and rounded edges. In the rock, the crystals

predominantly exhibit concave-convex contacts; however, straight contacts can be observed in inclusions and between recrystallized grains (Figure 5).

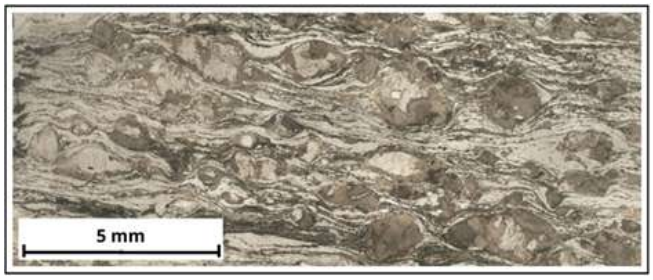

Figure 5 Integral image of a petrographic section of the studied mylonite, where the relationship between the porphyroblasts and the matrix can be observed in natural light.

5 Results

The results are divided into four parts: technological characterization, alterability, geochemistry, and reuse. The tests presented here followed the technical procedures established by the standards specified in Table 1. All data are derived from the characterization of the mylonite formed from the deformation of the migmatites belonging to the Granja Complex.

5.1 Technological Characterization

For the characterization of the mylonite, tests were conducted on compressive strength, flexural strength, impact resistance, slip resistance, abrasive wear resistance, determination of physical indices, and water absorption by capillarity. The Brazilian Association of Technical Standards (ABNT) establishes average behavior values for ornamental rocks extracted within the national territory according to standard NBR 15844. Although these average values do not represent minimum thresholds for a rock's market entry, obtaining results above these values necessarily indicates that the material exhibits physical-mechanical behavior above the average.

By associating above-average physical-mechanical parameters with uncommon aesthetic characteristics, one obtains an exotic and high-quality material. Such types of rocks are

typically the ones that achieve higher added value. In this context, all results obtained from the characterization of the mylonite were above the national average (Table 2).

In particular, low values for porosity, water absorption, and capillary absorption (which, as presented in Table 2, reach less than half of the national average limits) indicate a low interaction of the material with liquids. Considering that a large portion of pathologies are caused by substances in liquid form, it can be concluded that, since the rock has a low interaction with liquids, it also possesses greater resistance to the development of pathologies (Chiodi & Rodriguez 2009).

The slip resistance results indicate that the rock can develop very smooth surfaces when polished, suggesting that extra care is needed when the rock is used as flooring, especially if the surface of the slab is wet. The low values for abrasive wear indicate that the rock has high resistance to wear (Table 2), allowing it to be safely used in areas with high foot traffic.

When comparing the results obtained in this characterization with data from other aesthetically similar rocks already established in the market, such as Green Galaxy and

Table 2 Tests conducted in the technological characterization process and their respective results.

Technological Characterization				NBR 15844 (2010)
Tests		**Dry**	**Saturated**	
Flexural Strength (MPa)		21.6	17.46	≥ 10
Uniaxial Compressive Strength (MPa)		105	58	≥ 100
Slip Resistance		34.25	23.9	–
Amsler Abrasive Wear (mm)		500 m 0,26	1000 m 0.59	≥ 1
Physical Indices	Density (kg/m³)	2680.4		≥ 2550
	Porosity (%)	0.47		≤ 1.0
	Absorption (%)	0.18		≤ 0.40
Hard Body Impact Resistance (m)		0.35 m		≥ 0.3
Water Absorption by Capillarity		0.000145 g/cm² . s0.5		–

Verde Pantanal, it can be argued that the mylonite presented here has similar, and sometimes even superior, resistance parameters compared to these other rocks.

5.2 Alterability

To determine the rock's resistance to alteration, tests were conducted on chemical attack resistance, stain resistance, determination of the static contact angle with water, resistance to exposure to sulfur dioxide in humid conditions, and determination of the propagation speed of longitudinal waves.

The data obtained from these tests are useful for determining the best ways to utilize the rock in order to assist in its conservation. The chemical attack resistance test uses reagents of both basic and acidic nature found in various products to assess the rock's resistance to potentially aggressive substances. Among the reagents specified by NBR 16596, only hydrochloric acid and citric acid were able to cause significant changes in the mylonitic rock. In particular, hydrochloric acid has the ability to deepen fractures by dissolving the filling material (Figure 6).

The stain resistance test aims to understand the susceptibility of the rock's surface to develop non-removable stains. For the test, the rock is placed in contact with various everyday products for a period of 24 hours, after which the sample is cleaned with running water. These reagents were categorized into three classes: food products, non-food products from indoor environments, and non-food products from outdoor environments (Table 3).

Table 3 Reagents used in the stain resistance test.

Classes	Reagents	Character	Exposure
Food Products	Soy Sauce	Film Formation	24 hours
	Wine	Film Formation	24 hours
	Tomato Paste	Grease Action	24 hours
Non-food Products for Indoor Environments	Pen Ink	Film Formation	24 hours
	Mouthwash	Chemical action /oxidant	24 hours
	Vegetable Oil	Grease Action	24 hours
	Iodine Tincture	Chemical action /oxidant	24 hours
Non-food Products for Outdoor Environments	Automotive Oil	Grease Action	24 hours
	Uric Acid	Chemical action /oxidant	24 hours
	Steel Wool + Water	Chemical action /oxidant	24 hours

Of the 10 reagents, only 4 were able to generate irreversible stains on the rock: vegetable oil, steel wool, ink from a pen, and automotive oil (Figure 6). Since two of these reagents belong to the class of non-food products from outdoor environments, it can be concluded that the use of this rock presents a higher susceptibility to stain development when installed under these conditions.

The test for determining the static contact angle with water helps to understand the level of interaction of the rock's surface with Newtonian liquids; the greater the angle, the larger the area of contact between the liquid and the surface. In this context, a contact angle of 62° was obtained, indicating low hydrophobicity of the material and the need for surface waterproofing when exposed.

The propagation of longitudinal waves involves measuring the speed of P-waves to understand cohesion and estimate possible internal structures within a given material. The rock exhibits a wave propagation speed of 5850 m/s² when fully solid. According to Frazão & Farjallat (1995), the average wave propagation speed in rock is 4000 m/s²; thus, it can be concluded that the cohesion of the studied material is above average.

Finally, the test for exposure to sulfur dioxide in humid conditions, regulated by standard EN 13919, seeks to understand the rock's resistance to continuous exposure to SO_2- saturated environments, simulating a high-pollution atmosphere. The analyzed rock showed no changes in color parameters, nor in the physical parameters of porosity and water absorption, indicating a high resistance to the development of pathologies caused by a polluted atmosphere.

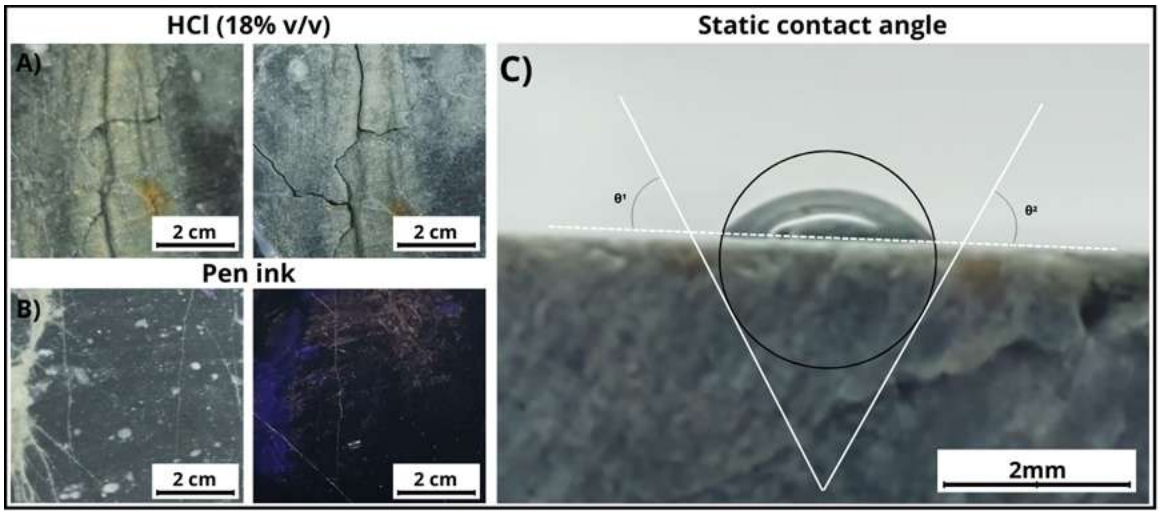

Figure 6 A. Image before and after treatment with 18% hydrochloric acid; B. Image before and after the staining test with paint; C. Static contact angle with water.

5.3 Geochemistry

To chemically characterize the studied rock, X-ray diffraction and ICP-OES analyses were performed on the whole rock. For the sample analysis, the samples were ground and sieved to a 200-mesh fraction. The diffraction analysis, complementary to the petrography, helped in identifying the most abundant mineral phases. The ICP-OES analysis not only aided in understanding the geochemical changes caused by mylonitization, but also provided a detailed composition of the rock to support its various uses.

The X-ray diffractometry analysis indicated the mineral phases corresponding to quartz, albite, K-feldspar, and biotite. Due to the small quantity, minerals with lower concentrations could not be identified. For the ICP-OES analysis, samples of both the studied mylonite and its protolith, the migmatite belonging to the Granja Complex, were used.

The results, presented in Table 4, demonstrate that the rock does not contain elements with potential environmental contamination. Furthermore, in the context of lithogeochemical comparison, variations in the contents of certain elements from the migmatite to the mylonite were identified, notably Ba, Sr, Fe, K, La, Li, Mg, Mn, and V. Changes in the quantities of Ba, Fe, and Ti may be associated with the comminution of biotite during the deformation process. Alterations in the contents of La, V, and Sr are attributed to changes in the abundance and composition of apatite. Meanwhile, the

decrease in the quantities of Fe and Mg is linked to a reduction in chlorite content with mylonitization.

Table 4 Lithogeochemical data of the mylonite and its protolith.

Lithogeochemistry	Migmatite	**B (% 10)**	**<0.1**	**W (ppm 50)**	**<50**	**Mn (ppm 10)**	**840**
		K (% 0.10)	1.71	As (ppm 30)	<30	Mo (ppm 10)	<10
		Ca (% 0.10)	1.92	Pb (ppm 20)	23	Nb (ppm 10)	<10
		Al (% 0.01)	6.92	Ba (ppm 10)	510	Ni (ppm 10)	37
		Fe (% 0.01)	4.4	Cd (ppm 10)	<10	Sr (ppm 10)	158
		Mg (% 0.01)	1.15	Co (ppm 10)	18	Ta (ppm 10)	<10
		P (% 0.01)	0.06	Cr (ppm 10)	183	V (ppm 10)	71
		Ti (% 0.01)	0.4	Cu (ppm 10)	<10	Zn (ppm 10)	67
		Sb (ppm 50)	<50	La (ppm 10)	27	Y (ppm 5)	18
		Sn (ppm 50)	<50	Li (ppm 10)	<10	Sc (ppm 5)	14
				Deformation			
	Mylonite	B (% 10)	<0.1	W (ppm 50)	<50	Mn (ppm 10)	317
		K (% 0.10)	2.99	As (ppm 30)	<30	Mo (ppm 10)	<10
		Ca (% 0.10)	1.51	Pb (ppm 20)	<20	Nb (ppm 10)	<10
		Al (% 0.01)	7.67	Ba (ppm 10)	962	Ni (ppm 10)	<10
		Fe (% 0.01)	2.04	Cd (ppm 10)	<10	Sr (ppm 10)	273
		Mg (% 0.01)	0.5	Co (ppm 10)	<10	Ta (ppm 10)	<10
		P (% 0.01)	0.09	Cr (ppm 10)	155	V (ppm 10)	24
		Ti (% 0.01)	0.31	Cu (ppm 10)	12	Zn (ppm 10)	52
		Sb (ppm 50)	<50	La (ppm 10)	48	Y (ppm 5)	9
		Sn (ppm 50)	<50	Li (ppm 10)	30	Sc (ppm 5)	<5

5.4 Reuse

The shape index, specific mass, and unit mass tests for the characterization of coarse aggregate yielded the following results: 2.5, 2.59 g/cm², and 1324 kg/m³, respectively. Since the material met the necessary requirements for use as aggregate, concrete test specimens were produced using substitution rates of crushed stone at 0%, 33%, 66%, and 100%. The 0% substitution represents a standard test specimen made without the presence of waste material.

The powdery material was separated using à 200-mesh sieve and used as an ecofiller, partially replacing cement in the concrete mix at a rate of 5%. To validate this as a form of reuse, concrete test specimens were made with ecofiller using the same composition as the mix previously determined.

After a curing period of 21 days, the test specimens produced with aggregate substitution and ecofiller were subjected to longitudinal wave propagation speed and uniaxial compressive strength tests. The values obtained from these tests indicate a strong similarity in the physical behavior of the concrete across all substitution rates adopted (Table 5). Thus, it is possible to conclude that the reuse of waste from the mylonitic rock, both in the form of ecofiller and as a replacement for coarse aggregate, is feasible.

Table 5 Characterization of concrete test specimens with the addition of mylonite waste.

Sample	Substitution Rate	Weight	Wave Speed	Propagation Time	Compressive Strength
Standard	0%	3.634	1549	45.4	33.60
2	33%	3.672	1577	44.4	27.96
3	66%	3.674	1570	44.6	32.70
4	100%	3.693	1613	43.4	32.57
Ecofiller	2%	3.630	1532	45.7	32.97

The portion of the waste characterized as fine aggregate (150 μm < x > 4.75 mm) was used to produce artificial stone. For the production of the samples, a composition of 70% stone and 30% resin was adopted. After the material cured for 72 hours, its physical indices and abrasive wear resistance were characterized.

The tests indicated that the artificial stone had density, porosity, and absorption values of 1882.37 kg/m³, 0.22%, and 0.12%, respectively. Regarding the Amsler wear resistance, values of 0.92 for 500 m and 1.77 for 1000 m were obtained, which indicates that this material is lighter than typical ornamental stones and has lower interaction with water. The observed results were similar to those obtained by Aguiar et al. (2017) and Lee et al. (2008) (Figure 7).

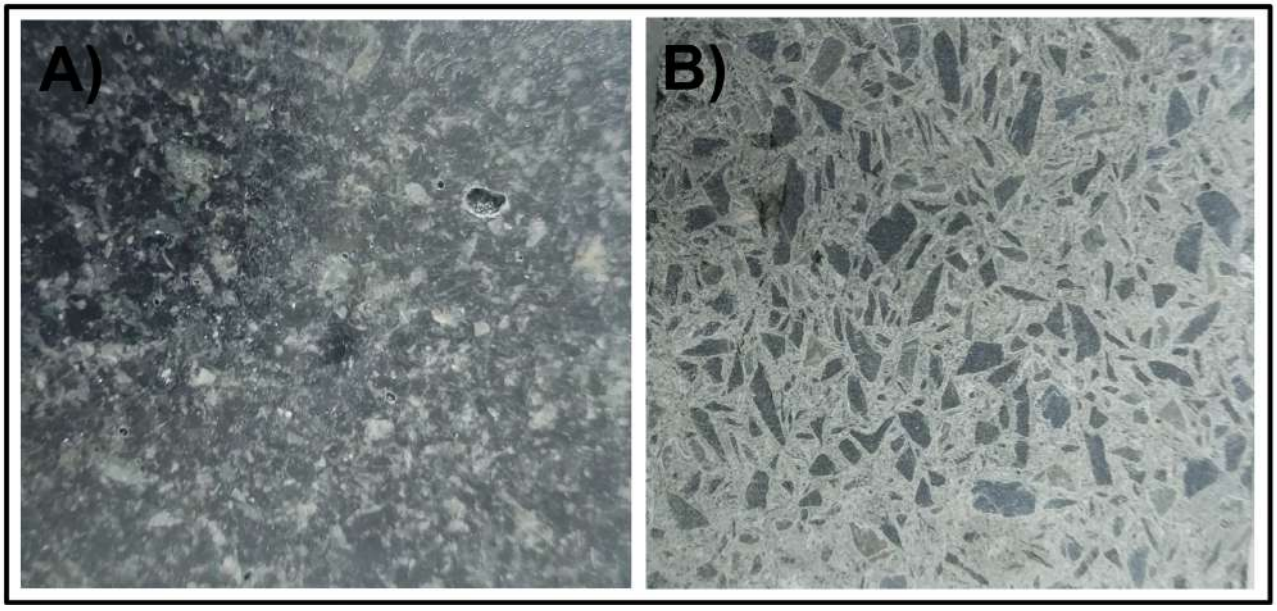

Figure 7 A. Macroscopic image of the conglomerated rock; B. Image before and after the staining test with paint.

6 Final Considerations

This work aimed to map and describe the mylonite belonging to the Granja Complex in the state of Ceará. The analyses conducted allowed for the characterization of the rock both for use as ornamental material and for the utilization of its waste in various applications. This integrated approach, which combines the determination of use with the reuse of waste, aligns with the principles of sustainable development.

Through geological field mapping, it was possible to identify that the studied rock resulted from the mylonitization of the migmatites of the Granja Complex due to movement in the Campanário Shear Zone. This mylonitization process also caused intense fracturing and low-temperature hydrothermal alterations in the adjacent rocks.

The mylonite exhibits gradations that range from unaltered rock to protomylonite and mylonite on an outcrop scale. This variation, coupled with the low rate of recrystallization observed, allows for the classification of the mylonite as low to medium grade. The rock shows a low incidence of microfractures, and the few fractures identified are related to neotectonic reactivations in the shear zone.

Regarding the physical-mechanical parameters, the main tests required by the Brazilian Association of Technical Standards (ABNT) for material characterization were carried out, in addition to complementary tests based on international standards. From these tests, a complete characterization of the studied rock was elaborated. The results obtained demonstrated that the rock performs better than the average parameters adopted nationally, qualifying it as a high-quality product. Furthermore, its dark green color, combined with the presence of white porphyroblasts that give the rock's texture a dynamic appearance, positions it as an exotic material with high added value in the ornamental rock market.

7 References

ABNT (Associação Brasileira de Normas Técnicas). 1987, *Agregados – Determinação da massa específica de agregados miúdos por meio do frasco Chapman*, NBR 9.776, Rio de Janeiro.

ABNT (Associação Brasileira de Normas Técnicas). 1992, *Materiais Inorgânicos - determinação do desgaste por abrasão*, NBR 12042, Rio de Janeiro.

ABNT (Associação Brasileira de Normas Técnicas). 2003, *Agregados – Determinação da composição granulométrica*, NBR NM 248, Rio de Janeiro.

ABNT (Associação Brasileira de Normas Técnicas). 2015a, *Rochas para Revestimento - Análise Petrográfica*, NBR NBR 15.845/1, Rio de Janeiro.

ABNT (Associação Brasileira de Normas Técnicas). 2015b, *Rochas para Revestimento – Densidade aparente, porosidade aparente e absorção de água - método de ensaio*, NBR 15.845/2, Rio de Janeiro.

ABNT (Associação Brasileira de Normas Técnicas). 2015c, *Rochas para Revestimento – Resistência à compressão uniaxial - método de ensaio*, NBR 15.845/5, Rio de Janeiro.

ABNT (Associação Brasileira de Normas Técnicas). 2015d, *Rochas para Revestimento - Determinação do Módulo de Ruptura (flexão por carregamento em três pontos)*, NBR 15.845/6, Rio de Janeiro.

ABNT (Associação Brasileira de Normas Técnicas). 2015e, *Rochas para Revestimento – Determinação da Resistência ao Impacto de Corpo Duro*, NBR 15845/8, Rio de Janeiro.

ABNT (Associação Brasileira de Normas Técnicas). 2015f, *Concreto – Procedimento para moldagem e cura de corpos de prova*, NBR 5738, Rio de Janeiro.

ABNT (Associação Brasileira de Normas Técnicas). 2017, *Rochas para revestimento – Determinação da resistência ao ataque químico – Método de ensaio*, NBR 16596, Rio de Janeiro.

ABNT (Associação Brasileira de Normas Técnicas). 2018, *Placas cerâmicas – Parte 14: Determinação da resistência ao manchamento*, NBR 10.545-14, Rio de Janeiro.

ABNT (Associação Brasileira de Normas Técnicas). 2019a, *Agregado graúdo – Determinação do índide de forma pelo método do paquímetro*, NBR 7809, Rio de Janeiro.

ABNT (Associação Brasileira de Normas Técnicas). 2019b, *Concreto endurecido – Determinação da velocidade de propagação de onda ultrassônica*, NBR 8802, Rio de Janeiro.

ABNT (Associação Brasileira de Normas Técnicas). 2021a, *Rochas ornamentais – Determinação da resistência ao escorregamento pelo método do pêndulo*, NBR 16959, Rio de Janeiro.

ABNT (Associação Brasileira de Normas Técnicas). 2021b, *Agregados – Determinação da massa unitária e do índice de vazios*, NBR 16972, Rio de Janeiro.

Agrizzi, C.P., Gadioli, M.C.B., Santos, E.A.C.C., Delaqua, G.C.G., & Vieira, C.M. F. 2019 'Produção e caracterização de rocha artificial com resíduos de quartizitos da lavra e beneficiamento de rochas ornamentais'. 74º Congresso Anual da ABM- Internacional, São Paulo.

Aguiar, M.C.D., Silva, A.G.P. & Gadioli, M.C.B. 2017, 'Rocha artificial produzida com pó de rocha e aglomerante polimérico'. 6th International Workshop Advances in Cleaner Production, São Paulo, Brasil, pp. 24-26.

ASTM (American Society for Testing and Materials). 2015, *Standard Test Method for Laboratory Determination of Pulse Velocities and Ultrasonic Elastic Constants of Rock*, ASTM D-2845, West Conshohocken.

Chiodi, F.C. & Rodrigues, E.D.P. 2009, *Guia de aplicação de rochas em revestimentos*,

Abirochas, São Paulo.

EN (Europeu de Normalização). 2010, *Conservation of cultural property - Test methods - Determination of static contact angle,* EN 15802, Bruxelas.

EN (Europeu de Normalização). 2003, *Natural stone test methods – Determination of resistance to ageing by SO2 action in the presence of humidity,* EN 13919, Bruxelas.

EN (Europeu de Normalização). 2000, *Natural stone test methods – Determination of water absorption coefficient by capillarity,* EN 1925, Bruxelas.

Frazão, E.B. & Farjallat, J.E.S. 1995, 'Seleção de pedras para revestimento e propriedades requeridas', *Revista Rochas de Qualidade*, 124.

Gesta, L.S.F., Santos, C.Q. & Souza, P.S.L. 2023 'Permeabilidade e microscopia de concretos com resíduo de corte de marmore e granito como filler'. Encontro Nacional de Aproveitamento de Resíduos na Construção, vol. 6, no. 1, pp. 616–628. Viewed 22 Out. 2024, https://eventos.antac.org.br/index.php/enarc/article/view/3439.

Lee, M. Y., Ko, C. H., Chang, F. C., Lo, S. L., Lin, J. D., Shan, M. Y. & Lee, J. C. 2008, Artificial stone slab production using waste glass, stone fragments and vacuum vibratory compaction', Cement and Concrete Composites, vol. 30, no. (7), pp. 583-587, DOI:10.1016/j.cemconcomp.2008.03.004.

Nunes, J.A.L., 2018, 'Caracterização litoestrutural de quartzitos da Serra do Mucuripe – NW do Ceará'. Master Dissertation, Universidade Federal do Ceará, Fortaleza. Viewed 22 Out. 2024, http://www.repositorio.ufc.br/handle/riufc/45392.

Pinéo, T.R.G. & Palheta, E.S.M., 2021 Projeto geologia e recursos minerais do Estado do Ceará: mapa geológico do estado do Ceará. Fortaleza: CPRM. Escala 1:500.000. 1 mapa, color. Viewed 02 Out 2024, https://rigeo.sgb.gov.br/handle/doc/20418.

Pinéo, T.R.G., Lima, A.F., Bessa, M.D.M.R. & Martins M.D. 2018. Projeto ARIM Noroeste do Ceará. Mapa Geológico-Geofísico: folha Bela Cruz - SA.24-Y-D- I.Estado do Ceará. Fortaleza: CPRM, 1 mapa colorido. Escala 1:100.000. Viewed 07 Sep. 2024, https://rigeo.cprm.gov.br/handle/doc/21399.

Queiróz, F.C. & Castro, N.F. 2017, 'Incorporação de resíduos de beneficiamento de rochas ornamentais em concreto autodensável como Ecofiller = Use of natural stones processing waste as Ecofiller in self-compacting concrete'. Jornada do Programa de Capacitação Interna do CETEM, 6. Rio de Janeiro. CETEM/MCTIC, pp. 31-37. Viewed 22 Out. 2024, http://mineralis.cetem.gov.br/handle/cetem/2077.

Santos, M.V., Oliveira, T.C.C. & Abreu, F.A.M. 2007, 'Regionalização de dados de cartografia geológica utilizando técnicas de Sensoriamento Remoto: o exemplo da Folha-Sobral-CE', XIII Simpósio Brasileiro de Sensoriamento Remoto. Florianópolis, pp. 2155-2161, INPE.

Silva, A.J.F., 2017, 'Processos de Migmatização no Complexo Granulítico de Granja: Domínio Médio Coreaú, Ceará, Brasil', PhD. Thesis, Universidade de Aveiro, Portugal.

Author contributions
Davi Henrick Veras Diógenes: conceptualization; formal analysis; methodology; validation; writing-original draft; visualization. **Irani Clezar Mattos:** methodology; validation; writing – review and editing; supervision.

Conflict of interest
The authors declare no conflict of interest.

Data availability statement
All data included in this study are publicly available in the literature.

Funding information
Not applicable.

Editor-in-chief
Dr. Claudine Dereczynski

Associate Editor
Dr. Márcio Fernandes Leão

How to cite:
Diógenes, D.H.V., & Mattos, I. C. 2025, 'Geological and Industrial Characterization of the Mylonite Belonging to the Granja Complex, Morrinhos - CE', *Anuário do Instituto de Geociências,* 48:66134. https://doi.org/10.11137/1982-3908_2025_48_66134